Quantum CART (*qCART*), a *piggyBac*-based system for development and production of virus-free multiplex CAR-T cell therapy

Yi-Chun Chen[1], Wei-Kai Hua[1], Jeff C. Hsu[1], Peter S. Chang[1], Kuo-Lan Karen Wen[1], Yi-Wun Huang[1], Jui-Cheng Tsai[1], Yi-Hsin Kao[1], Pei-Hua Wu[1], Po-Nan Wang[2], Ke-Fan Chen[1], Wan-Ting Liao[1], Sareina Chiung-Yuan Wu[1,†]

[1]GenomeFrontier Therapeutics, Inc. Taipei City, Taiwan (R.O.C.)

[2]Division of Hematology, Chang Gung Medical Foundation, Linkou Branch, Taipei City, Taiwan (R.O.C.)

[†]Correspondence should be addressed to:

S.C.-Y.W. (sareina@genomefrontier.com) 23F., Building C, No. 95, Sec. 1, Xintai 5th Rd., Xizhi Dist., New Taipei City 221416, Taiwan (R.O.C.); +886-2-26558766;

Keywords: multiplex; CAR-T; *piggyBac*; T_{SCM}; transposon

Abstract

Chimeric antigen receptor T (CAR-T) cell therapy has the potential to transform cancer treatment. However, CAR-T therapy application is currently limited to certain types of relapsed/refractory B cell lymphomas. To unlock the full potential of CAR-T therapy, technologic breakthroughs will be needed in multiple areas, including optimization of autologous CAR-T development, shortening the innovation cycle, and further manufacturing advancement of next-generation CAR-T therapies. Here, we established a simple and robust virus-free multiplex *Quantum CART*™ system that seamlessly and synergistically integrates four platforms: 1. *GTailor*™ for rapid identification of lead CAR construct design, 2. *Quantum Nufect*™ for effective but gentle electroporation-based gene delivery, 3. *Quantum pBac*™, featuring a virus-free transposon-based vector with large payload capacity and integration profile similar to retrovirus, and 4. *iCellar*™ for robust and high-quality CAR^+ T memory stem cell expansion. This robust, virus-free multiplex *Quantum CART*™ system is expected to unleash the full potential of CAR-T therapy for treating diseases.

36 **Introduction**

37 In recent decades, immunotherapy involving T lymphocytes capable of
38 antigen-specific recognition leading to cytotoxic activity and persistence, have
39 taken center stage in tumor eradication.[1,2] Among T cell-based therapies, chimeric
40 antigen receptor T (CAR-T) therapies that combine the specificity of antibody
41 recognition and T cell activating functions into a single protein receptor, have
42 shown considerable potential to advance cancer treatment.[3] [4]

43 A successful CAR-T therapy requires not only tumor recognition, but also
44 sufficient cell expansion, persistence, and delivery of effector functions. Second
45 generation CAR-T cells that incorporate CD28 or 4-1BB in the CAR design have
46 demonstrated therapeutic efficacy against hematological malignancies.[5] However,
47 successful treatment against solid tumors remains a challenge due to the hostile
48 immunosuppressive tumor microenvironment (TME) that inhibits the infiltration,
49 survival, and cytotoxic activity of CAR-T lymphocytes.[6–8] One strategy to
50 overcome this challenge is to engineer CAR-T cells to express additional genes
51 that enhance CAR-T functions, so called armored CAR-T cells.[9] Efficacy of
52 armored CAR-T therapies against solid tumors in preclinical studies has been well-
53 documented, and clinical trials are currently ongoing.[10–15] However, the repertoire
54 of genes that can be included in armored CAR-T therapies has been severely
55 restricted by the limited cargo capacity of viral vectors. Another strategy is to
56 enrich for specific T cell subsets that possess superior capability to persist and
57 attack cancer. Ever since Gattinoni *et al.* described memory stem T cells (T_{SCM}),[16]

58 several studies have demonstrated T_{SCM} to be critical in facilitating successful
59 adoptive T cell therapy.[17–20]

60 Currently, retroviral and lentiviral vectors are the most common vehicles used
61 for CAR-T engineering.[21,22] However, virus-based CAR-T therapies have potential
62 risk of genotoxicity and are unsuitable for multiplex CAR-T production due to
63 limited gene cargo capacity. Furthermore, the high cost of virus-based CAR-T
64 therapies prevent widespread patient accessibility. Non-virus-based CAR-T
65 therapy is a promising alternative. However, until more recently its development
66 has been hampered by low gene transfer efficiency and difficulty to efficiently
67 expand quality engineered T cells for clinical application.[23]

68 In this study, we describe virus-free *Quantum Engine*™, a cell engineering
69 and production system composed of four platforms: *GTailor*™, *Quantum Nufect*™,
70 *Quantum pBac*™, and *iCellar*™. We demonstrate that *qCART*™ (a *Quantum*
71 *Engine*™ for CAR-T production) can generate multiplex CAR-T cells that express
72 genes of interest (GOIs) with various targeting specificities and sizes. The
73 engineered CAR-T cells consistently exhibit desired features, including high T_{SCM},
74 high expansion capacity, and robust anti-tumor efficacy.

75 Given that *qCART*™ can shorten both the development and manufacturing
76 timeline of virus-free multiplex CAR-T therapy, *qCART*™ represents a

77 technological breakthrough that will be expected to unlock the full potential of CAR-
78 T therapies and facilitate widespread patient access.
79
80 **Results**
81 ***GTailor*™ facilitates screening of therapeutic gene constructs to identify lead**
82 **candidates for preclinical development**
83 Since identification of CAR-T lead candidates is laborious, time-consuming
84 and requires multiple rounds of screening involving designing and construction of
85 gene constructs and subsequent *in vitro* and/or *in vivo* testing and validation, we
86 developed the *GTailor*™ platform to streamline these processes for efficient lead
87 candidate identification. This platform consists of the following technologies: (1) a
88 library of functional modules for rapid establishment of a therapeutic construct, (2)
89 a simple, time-effective and economical cell engineering process for building a
90 multiplex CAR-T cell library, (3) a high throughput *in vitro* cytotoxicity assay system
91 for identifying potent, persistent CAR-T cells that possess high On-Target, and
92 minimal Off-Tumor toxicities. A sample screening process for B-cell maturation
93 antigen (BCMA) CAR-T cells is depicted in Supplementary Fig. S1, and the results
94 are presented in Table 1. As shown, all five groups of CAR-T cells performed
95 similarly and satisfactorily in terms of cell expansion (day 1 to 10-fold change),
96 percentage of CAR^+ cells, CD8/CD4 ratio, and percentage of T_{SCM} in both CD4
97 and CD8 populations (Table 1).
98
99

100 **Table 1. Finding optimal BCMA CAR-T cells**

101 Human peripheral blood mononuclear cells (PBMC) electroporated with *Quantum pBac*™
102 expressing anti-BCMA CARs were analyzed for their performance, including cell expansion (Day 1
103 to 10 fold change), percentage of CAR^+ cells, CD8/CD4 ratio, percentage of T_{SCM} cell subsets in
104 $CD4^+$ or $CD8^+$ cells, and cytotoxicity against $BCMA^+$ cells. Data shown are from four healthy donors.
105 Results are shown as mean fold change, CD8/CD4 ratio, cytotoxic activity, or percentage of CAR^+,
106 $CD4^+/T_{SCM}$, $CD8^+/T_{SCM}$, or $CAR^+/PD1^+$ cells.

Group	N (independent experiments)	Day 1 to 10 fold change	% CAR^+	CD8/CD4 ratio	% T_{SCM} in $CD4^+$	% T_{SCM} in $CD8^+$	% $PD1^+$ in CAR^+	Cytotoxicity against $BCMA^+$ cells (5:1, 48hr)
aBCMA-1	2	168 (101, 236)	45.8 (45.0, 46.6)	1.3 (0.9, 1.7)	60.3 (59.5, 61.1)	74.6 (73.3, 75.9)	NA	15.8 (14.7, 16.8)
aBCMA-2	7	226 (141~384)	63.7 (55.3~74.5)	1.5 (0.4~3.8)	71.0 (63.3~80.6)	76.3 (63.3~83.1)	0.8 (0.6~1.7)	55.3 (46.0~71.5)
aBCMA-3	3	289 (162~472)	51.6 (33.9~73.4)	2.7 (1.4~4.2)	76.6 (67.6~84.7)	82.4 (754~87.4)	74.6 (49.9~90.4)	9.8 (3.3~14.2)
aBCMA-4	2	223 (149, 297)	57.8 (50.5, 65.1)	3.4 (1.8, 5)	68.1 (64.9, 71.3)	69.5 (57.4, 81.6)	6.4 (1.2, 11.5)	12.5 (11.7, 13.2)
aBCMA-5	3	278 (187~454)	68.3 (68.1~68.5)	2.5 (1.9~3.7)	73.6 (67.1~80.4)	79.7 (71.7~85.7)	0.6 (0.4~ 1.1)	50.5 (43.2~57.5)

107
108

109 However, three CAR-T groups (aBCMA-1, aBCMA-3 and aBCMA-4)
110 exhibited markedly lower cytotoxicity against $BCMA^+$ target cells. Note that the
111 percentage of $PD1^+$ CAR-T cells in the aBCMA-3 group was also markedly higher
112 than those found in other groups. CAR-T cells with these undesired traits were
113 tested at least twice (using T cells derived from different donors), whereas other
114 groups were tested at least three times to confirm reproducibility. As a result,
115 aBCMA-2 and aBCMA-5 CAR-T cells were identified as tentative candidates.
116 These two candidate CAR-T groups were next co-cultured with a panel of BCMA-
117 negative and BCMA-positive tumor and normal cells. As shown (Supplementary

118 Table S1), aBCMA-5 lysed more cells expressing minimal BCMA, therefore
119 aBCMA-2 was chosen as the candidate for pipeline development.

120 ***Quantum pBac*™ (*qPB*) facilitates consistent intra-cell type genome**
121 **integration**

122 We have previously demonstrated that the *qPB* system is superior
123 compared to other *piggyBac* transposon systems.[24] Since the integration
124 characteristics of *qPB* is unknown, we analyzed for the first time, the integration
125 profile of *qPB* in CAR-T cells. Additionally, we compared the integration profile
126 with that of human embryonic kidney (HEK293) cells[25] to determine whether there
127 may be any inter-cell type differences. As shown in Figure 1A, integration sites
128 (IS) were identified within all T cell chromosomes with the exception of

129 chromosome Y. This may be due to the relatively smaller size of Y chromosome,

130 and would be consistent with the lower number of IS found within relatively smaller

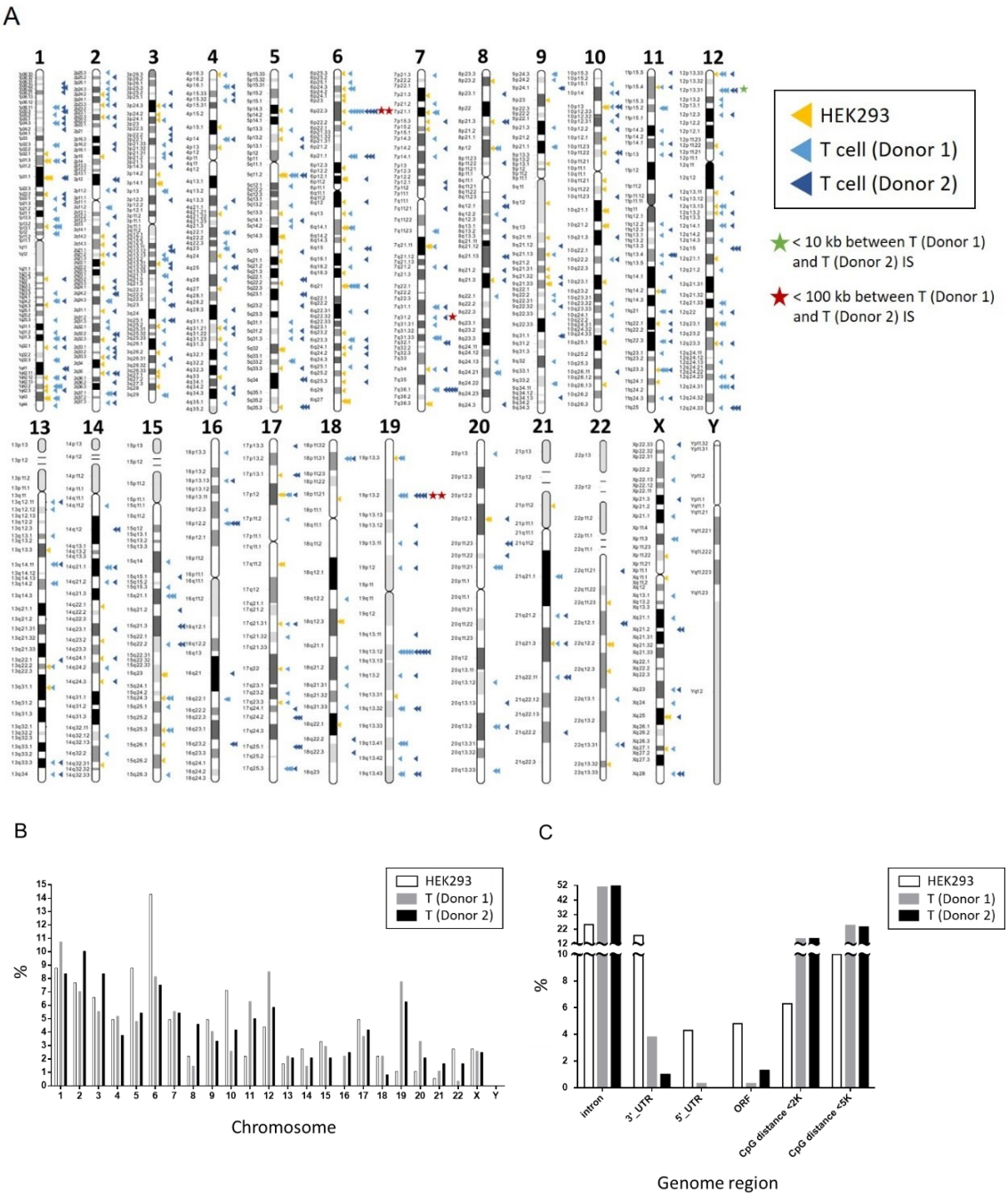

131

132 **Figure 1. Profiling of *Quantum pBac*™ (*qPB*) genome integration**

133 (A) A schematic depiction showing the biodistribution of *qPB* genome integration sites (IS) mapping
134 to specific segments of the indicated HEK293 and primary T cell chromosomes. (B), (C) IS as
135 shown in (A), data analyzed and grouped by: the indicated chromosome (B), and the indicated
136 genome region (C). Results shown are from two females (HEK293, T donor 2) and one male (T
137 donor 1), and results of (B) and (C) are presented as percentages of total IS.
138

139 chromosomes such as chromosomes 13-22 (Figure 1A and 1B). In contrast to the
140 relatively consistent IS biodistribution pattern found in T cells derived from two
141 separate donors, several distinct differences were found in integration profile
142 between HEK293 and T cells. For example, in contrast to T cells, no IS were found
143 within chromosome 16 of HEK293 (Figure 1A and 1B). Moreover, higher
144 percentages of IS were found within chromosomes 5 and 6 of HEK293, whereas
145 more IS were found within chromosome 19 for T cells (from both donors; Figure
146 1B).

147 Since *qPB* genome insertion may raise safety concerns, we next analyzed
148 the biodistribution of IS within or near different areas of genes. A total of 344 and
149 300 unique IS were identified within CAR-T cell donor 1 and donor 2, respectively
150 (Supplementary Table S2). Of note, we observed that increasing the amount of
151 donor DNA (carrying CAR) introduced into CAR-T cells increases integrant copy
152 number in cells.[26] To reduce safety risks, we optimized the concentration of donor
153 DNA such that integrant copy number per cell would be below five, as shown by
154 the low CAR copy numbers found in T cells of both donors (3.08 and 1.68 in donors
155 1 and 2, respectively; Supplementary Table S2). Interestingly, remarkable
156 conformity was found in the integration profiles of both donor T cells. For example,

157 approximately 50% of IS (50.9% and 52% in donors 1 and donor 2, respectively)
158 were found in the introns, while a very low percentage (0.3% and 1.3% in donors
159 1 and donor 2, respectively) were found in the open reading frame (ORF) of protein
160 coding gene (Figure 1C). Historical data demonstrated that lentiviral vector with
161 an even higher percentage (79.7%) of intronic IS[27] is considered to be relatively
162 safe. This suggests that *qPB* may be as safe as lentiviral vectors, although other
163 factors including bias concerning targeting genes and transcriptional start
164 sites/termination sties remain to be assessed. Furthermore, the lower percentage
165 of IS found in the introns (25.2%) and higher percentage of IS found in the ORF
166 (4.8%) of HEK293 cells support cell type-specific biodistribution of *qPB* IS. Next,
167 we focused on IS in the CpG dinucleotide-rich regions (CpG islands) since the
168 transcription of >50% of human genes are initiated from these regions.[28] Similar
169 percentages of IS were found <5 Kb from CpG islands (24.7% and 23.7% in donors
170 1 and donor 2, respectively) as compared to published data in cells transduced
171 using retrovirus (32.8%) or hyperactive *piggyBac* (*hyPB*, 26.6%).[27].

172 While the majority of IS were identified in genes, none of the top 10 IS of
173 either T cell donors targeted within known cancer-associated genes
174 (Supplementary Table S3). Importantly, some IS were found within or in proximity
175 to cancer-associated genes, but they were either in the intronic region, in the UTR
176 region, or upstream of these genes (Supplementary Table S4). Moreover, no IS
177 was found in/near any of the genes (*CCND2, HMGA2, LMO2, MECOM, MN1,*
178 *PRDM16*) previously reported to be associated with severe adverse events in

179 patients.[29–32] This biodistribution pattern of IS thereby suggests that *qPB* may be
180 as safe as currently available randomly-integrating vector systems.

181 ***Quantum Nufect*™ (*qNF*) facilitates effective transfection of human primary**
182 **T cells while preserving high cell viability**

183 Electroporation is the most efficient method for delivery of virus-free vectors
184 into therapeutic cells. However, a major bottleneck of this approach includes low
185 viability and expansion capacity of electroporated cells. To address this matter,
186 we developed a cell type-independent generic buffer system for electroporation
187 called *Quantum Nufect*™ (*qNF*). We utilized Lonza's Nucleofector™ to assess the
188 effect of *qNF* on T cell transfection efficiency. We first nucleofected T cells with a

189 pmaxGFP plasmid using *qNF*, and compared the results to those obtained using

190 the Human T Cell Nucleofector™ Solution (HTCN, Lonza; Figure 2A).

191

192

193

194

195

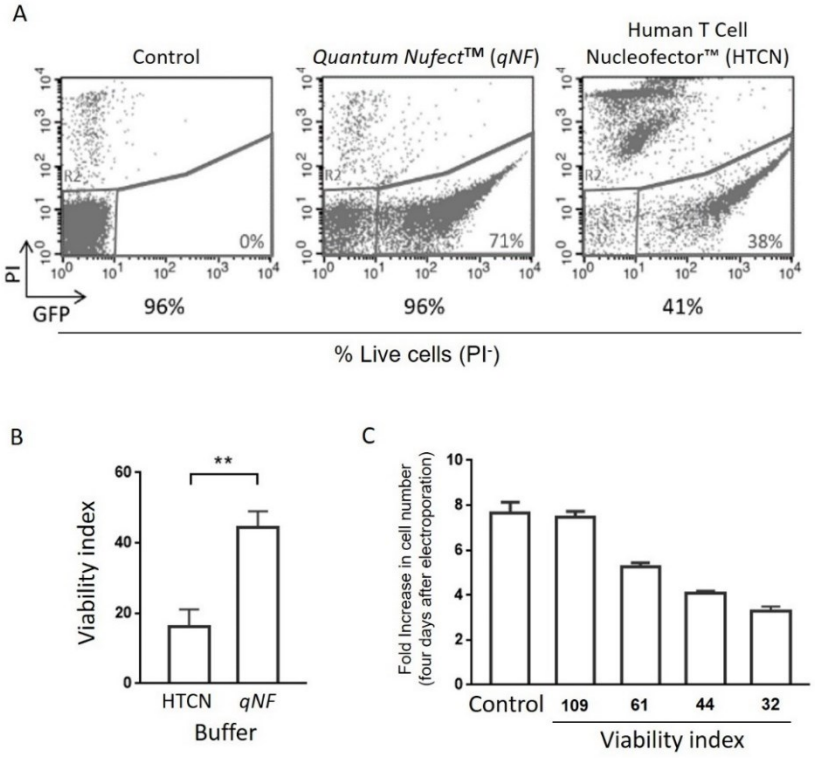

196

197

198

199

200

201

202 **Figure 2. Viability of human primary T cells electroporated using *Quantum Nufect*™ (*qNF*)**

203 **and compared with those electroporated using the Human T Cell Nucleofector™ solution**

204 Human peripheral blood CD8⁺ T cells electroporated with pmaxGFP plasmid in either *qNF* buffer

205 or Human T Cell Nucleofector™ (HTCN) solution. One day after electroporation, transfected cells

206 were analyzed for (A) GFP and PI staining, and (B) viability index. (C) Human peripheral blood T

207 cells electroporated under conditions that result in different levels of post-electroporation viability

208 were analyzed for their viability indices plotted versus fold increase in cell number after four days

209 of culture. Results are shown as percentage of cells positive or not positive for GFP and/or PI

210 staining (A), mean viability index (B, C) and the mean fold increase in number of cells (C). ** $p <$

211 0.01. N = 3 (B, C, triplicates).

212

213 We show in a representative experiment, that unlike the low viability (41%)
214 seen in HTCN-transfected T cells, *qNF* preserved the viability of a high percentage
215 (96%) of cells at a level comparable to non-nucleofected control cells. These
216 results are consistent with a significantly higher viability index in *qNF*-nucleofected
217 cells (Figure 2B). We next examined the relationship between cell viability and
218 expansion capacity of T cells transfected with pmaxGFP using *qNF*. As shown in
219 Figure 2C, low initial viability resulted in low subsequent expansion after three
220 additional days of culture, suggesting that cell viability following nucleofection is
221 positively associated with cell expansion capacity.

222 Next, we assessed the effect of *qNF* on CAR transfection efficiency by
223 nucleofecting cells with *qPB* carrying a transcript expressing a tandem CD20/CD19
224 CAR, and iCasp9, using *qNF* or HTCN. As shown in Figure 3A, significantly more
225 total live cells were recovered from the *qNF* group (8.9E5 ± 9.3E4) compared with
226 those recovered from the HTCN group (3.2E5 ± 1.0E5) one day after
227 nucleofection. While a significantly higher percentage of live cells of the HTCN
228 group were CAR^+, nearly twice as many CAR^+ T cells were recovered using *qNF*
229 (2.0E5 ± 3.7E4) compared to that using HTCN (1.2E5 ± 3.8E4; Figure 3A).

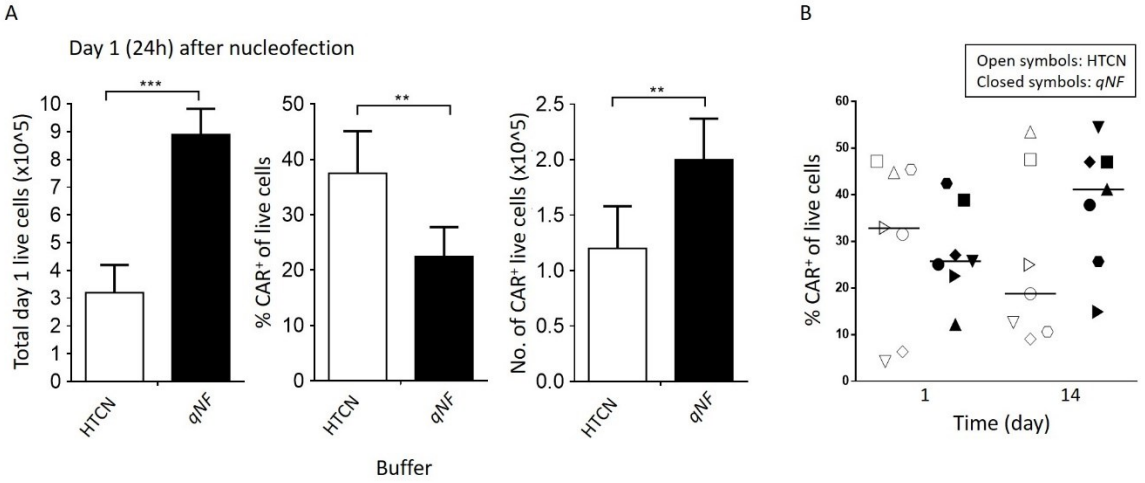

230

231 **Figure 3. Human primary T cells electroporated using *Quantum Nufect*™ (*qNF*) buffer**
232 **system produces high yield of CAR⁺ T cells**

233 Human peripheral blood T cells electroporated with *Quantum pBac*™ expressing CAR in either
234 *qNF* buffer or Human T Cell Nucleofector™ (HTCN) solution were harvested one day after
235 electroporation and analyzed for (A) CAR and PI staining, and yield calculation. (B) The
236 percentages of CAR⁺ cells were analyzed on day 1 and day 14. Results are shown in (B) as median
237 percentage of CAR⁺ live cells. Yield is calculated as No. of CAR⁺ live cells, using the formula: (Total
238 day 1 live cells) × (percentage of CAR⁺ live cells). ** $p < 0.01$, *** $p < 0.001$. N = 3 (A, triplicates),
239 N = 7 donors (B).

240

241 Next, we addressed whether the greater transfection rate seen in HTCN-
242 transfected cells would result in higher percentage of CAR⁺ cells in the final CAR-
243 T product. We compared CAR transfection efficiency using *qNF* vs HTCN in cells
244 obtained from seven healthy donors. As shown in Figure 3B, despite an initial
245 lower percentage of CAR⁺ T cells one day after nucleofection using *qNF*, there
246 was an overall increase in CAR⁺ cells after 14 days of culture. This is in contrast
247 to an overall decrease in percentage of CAR⁺ cells seen in T cells nucleofected

248 using HTCN. In fact, in cells from five out of seven donors, the slope of increase
249 in percentage of CAR^+ T cells following nucleofection was steeper in *qNF* than in
250 HTCN-nucleofected cells (Supplementary Fig. S2). Moreover, in the remaining
251 two donors, the slope of decrease in percentage of CAR^+ T cells following
252 nucleofection was the same or less steep in *qNF* than in HTCN-nucleofected cells.
253 These evidence suggest that an initial high percentage of CAR^+ cells will
254 not always lead to high CAR^+ cell enrichment at harvest, and that *qNF* is superior
255 and more reliable in producing and enriching for CAR^+ T cells than HTCN.

256 ***iCellar*™ robustly enriches and expands CAR-T cells while maintaining cell**
257 **stemness (T_{SCM})**

258 We have previously shown that *qPB* can be advanced towards clinical
259 application in CAR-T therapy.[24] However, even in the presence of artificial antigen
260 presenting cells (aAPC), T cells from some donors still failed to sufficiently expand.
261 To resolve this issue, we developed a CAR-T cell culture supplement named
262 *Quantum Booster*™ (*qBT*), which in conjunction with aAPC are both components
263 of *iCellar*™. We analyzed the effect of *iCellar*™ on performance of CAR-T cells
264 by determining whether different components of *iCellar*™, namely aAPC, *qBT*, or
265 their combination (aAPC+*qBT*), affect the characteristics of CAR-T cells produced.
266 As shown in Figure 4, *qBT* increased the expansion of CAR-T cells (Figure 4A), as
267 well as significantly enriched for CAR^+ T cells (Figure 4B).

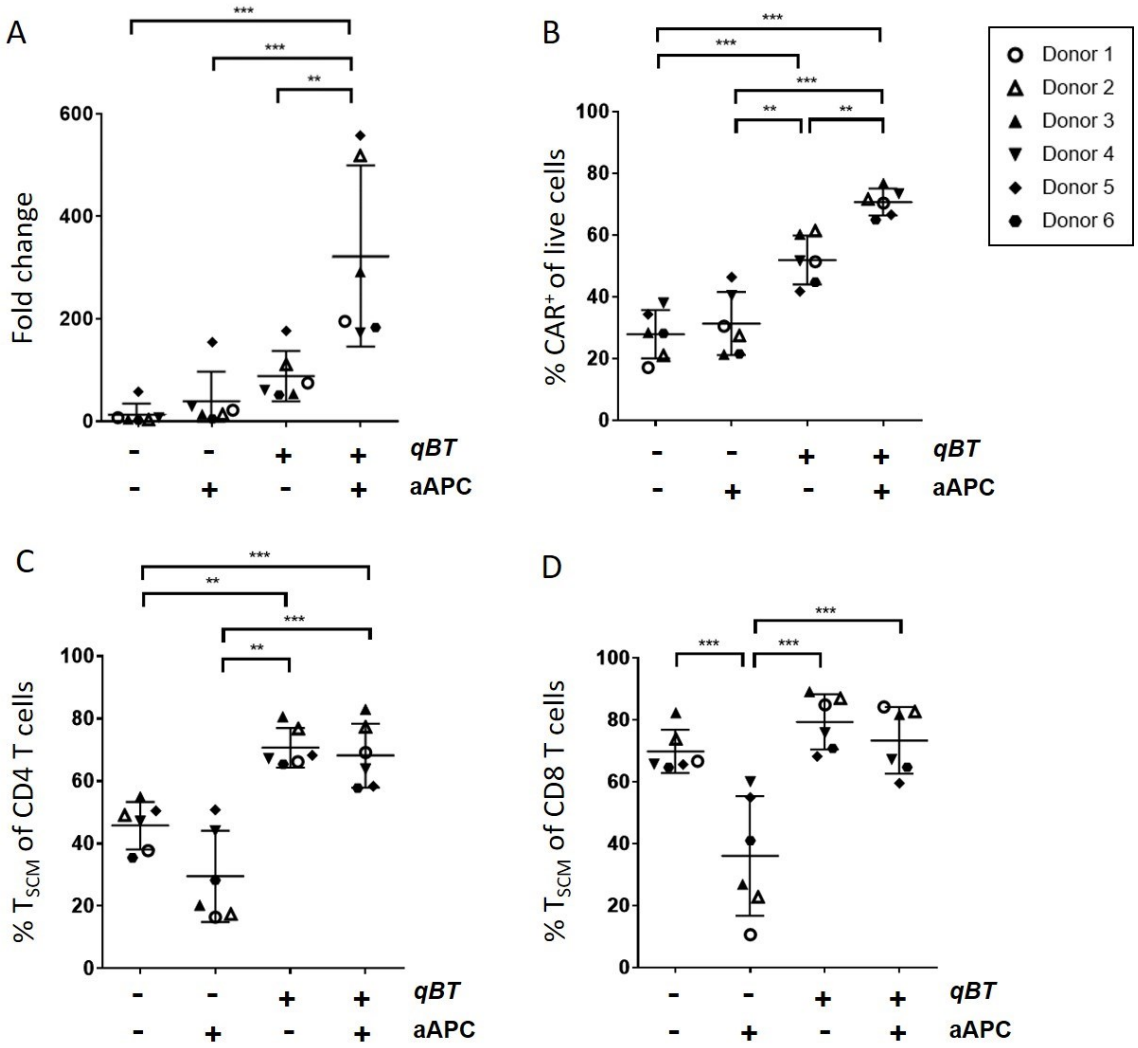

268

269 **Figure 4. The effect of different *iCellar*™ combinations on characteristics of CAR-T cells**

270 Human peripheral blood mononuclear cells (PBMC) electroporated with *Quantum pBac*™

271 expressing CAR and cultured for 10 days in the presence or absence of aAPC and/or *Quantum*

272 *Booster*™ (*qBT*) were harvested and assessed for (A) cell expansion fold change, (B) percentage

273 CAR^+ of live cells ($CD3^+$ PI^-, >90%), and percentage of T_{SCM} cell subsets in (C) $CD4^+$ or (D) $CD8^+$

274 cells. Data shown are from six healthy donors. Horizontal lines represent the mean and s.e.m. fold

275 change (A), mean and s.e.m. percentage of CAR^+ cells (B), and mean and s.e.m. percentage of

276 T_{SCM} cell subsets (C and D). * $p < 0.05$, ** $p < 0.01$, *** $p < 0.001$.

277

278 On the other hand, while aAPC alone did not significantly affect expansion
279 or percentage of CAR^+ T cells, aAPC+*qBT* significantly enhanced both of these
280 parameters (Figure 4A and 4B). Moreover, while either *qBT* or aAPC+*qBT*
281 increased the percentage of T_{SCM} cells over the control group (Figure 4C and 4D),
282 aAPC alone markedly decreased the percentage of T_{SCM} cells. This effect, which
283 reached statistical significance in the $CD8^+$ population (Figure 4D) suggests that
284 aAPC promotes cell maturation. Furthermore, aAPC+*qBT* significantly blocked the
285 reduction in percentage of T_{SCM} cells (Figure 4C and 4D), suggesting that *qBT*
286 maintains cells in a less differentiated state (i.e. T_{SCM}). These results demonstrate
287 that *qBT* of *iCellar*™ markedly enhance the expansion capacity of CAR-T cells
288 while preserving and/or even enhancing CAR-T quality.

289 **Effective tumor clearance by *qCART*™-produced CAR-T cells in Raji-bearing**
290 **immunodeficient mice**

291 To further determine the effect of aAPC on the functionality of *qCART*™-
292 produced CAR-T cells, we first assessed its effect on the performance of CAR-T
293 cells produced from four healthy donors (Supplementary Table S5). We found
294 similar and consistent performance in cells from all four donors, and assessed
295 cytotoxic activities of T cells from donor A. As shown in Figure 5A, CAR-T cells
296 effectively lysed Raji-GFP/Luc cells.

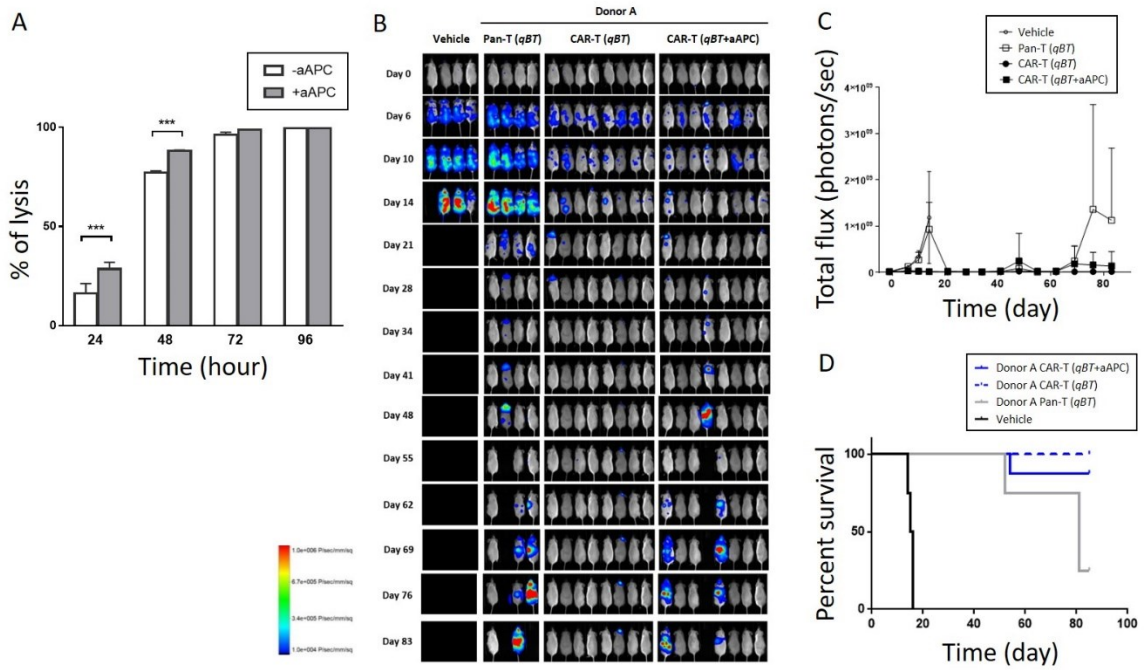

Figure 5. *In vitro* and *in vivo* functional characterization of CAR-T cells produced using the *qCART*™ system

(A) *In vitro* cytotoxicity of CAR-T cells (E:T ratio of 1:1) with or without pre-incubation with aAPC, on Raji-GFP/Luc target cells. (B) *In vivo* cytotoxicity of CAR-T cells with or without pre-incubation with aAPC in Raji-GFP/Luc-bearing immunodeficient mice. Fluorescence intensity values (C) and survival curves (D) of mice from (B) plotted against time. Results shown are from four to eight mice/group. T cells were obtained from a representative donor. Vehicle and Pan-T cells (non-engineered T cells) were used as controls. *Quantum Booster*™ (*qBT*) was present in all cell culture conditions. *** $p < 0.001$.

Of note, CAR-T cells expanded with aAPC exhibited significantly increased killing efficacy at earlier (24h and 48h) time points. In contrast to vehicle and pan-T-injected mice, Raji-bearing mice injected with CAR-T cells (*qBT* or *qBT*+aAPC) killed markedly more Raji cells (Figure 5B, 5C), despite the significantly higher

312 plasma IFN-γ levels in pan-T-injected mice (Supplementary Fig. S3A, see day 15).
313 The superior antitumor efficacy of CAR-T cells either with *qBT* or *qBT*+aAPC was
314 also shown by the prolonged survival of these mice compared with those injected
315 with vehicle or pan-T cells (Figure 5D). This observation is consistent with the
316 absence on day 85, of detectable Raji cells remaining in the blood and bone
317 marrow of CAR-T treated mice (*qBT* or *qBT*+aAPC; Supplementary Fig. S3C),
318 despite the continued presence of tumor in the liver and/or ovaries of tumor-
319 bearing mice (Figure 5B, Day 83, CAR-T (*qBT*+aAPC); verified by surgery).
320 Interestingly, we observed tumor relapse in mice that had been injected with CAR-
321 T cells cultured with *qBT*+aAPC, but not with *qBT* alone. We also observed that
322 in one mouse (first from the left in the "CAR-T (*qBT*)" panel) tumor relapsed by day
323 21. However, complete tumor remission was again observed by day 34 with no
324 further evidence of relapse up end of experiment (Figure 5B). This observation is
325 corroborated by the expected higher number of circulating CAR^+ T cells (due to
326 higher CAR copy number in blood) found in CAR-T cell-treated mice on day 71 vs
327 day 43 (Supplementary Fig. S3B), and suggests that the increased CAR^+ T cells
328 may contribute to tumor clearance.

329 ***qCART*™ produces CAR-T cells of different targeting specificity and gene of**
330 **interest sizes with expansion capacity capable of reaching clinical scale**
331 **production**

332 To determine whether CAR-T cells with CAR genes expressing binder(s)
333 against various antigens and/or transgene of various sizes could be effectively
334 generated, we nucleofected *qPB* carrying various genes of interest (GOI) into T

335 cells of healthy donors and analyzed the performance of CAR-T cells. Using the
336 perfusion setup, we observed that increasing the transgene size decreased the
337 percentage and expansion capacity of CAR^+ cells (Supplementary Table S6). On
338 the other hand, using the G-Rex setup, even though we still observed an inverse
339 association between percentage of CAR^+ cells and GOI sizes, the difference in
340 CAR^+ cell expansion appeared to be more consistent and much less affected by
341 GOI size (Table 2).

342 **Table 2. Consistent performance of CAR-T cell products produced by *qCART*™**

Pipeline (Multiplex)	GOI Size (Kb)	Description	% CAR^+	CAR-T Expansion (Fold Increase)	CD8/CD4 Ratio	% $CD8^+$ T_{SCM}/ % $CD4^+$ T_{SCM} in CAR^+	Exhaustion Markers PD-1/ TIM3/ LAG3 (%)	Senescence Markers KLRG1/ CD57 (%)	Representative *In Vitro* Cytotoxicity (%)
GF-CART01 (CD20/CD19-iCasp9)	5.2	iCasp9 + CD20/CD19	31.9~49.9 (n=6)	158~512	5	73.6~94.7/ 65.1~82.5	0.4~2.0/ 0.0~5.3/ 0.9~7.0	2.2~14.6/ 0.0~0.7	32.7~92.8 (E/T=1, 48 hrs)
GF-CART02 (Dual CAR-iCasp9) Multiple Myeloma	3.4	CAR (binder 1)	55.3~74.5 (n=7)	141~383	0.4~3.8	63.3~83.1/ 63.3~80.6	0.2~1.7/ 0.5~7.6/ 0.6~3.4	0.4~7.9/ 0.2~10.8	41.6~71.3 (E/T=5, 48 hrs)
	3.4	CAR (binder 2)	44.4~88.7 (n=4)	163~535	1~3.5	74.4~79.2/ 53.3~71.3	0.2~3.6/ 0.8~4.2/ 0.9~4.5	7.8~24.5/ 0.1~1.2	19.3~39.1 (E/T=5, 48 hrs)
	5.4	iCasp9-CAR (binder 1+2)	48.4, 58.5 (n=2)	134, 243	1.8, 1.8	68.8, 72.2/ 75.6, 75.7	0.2, 0.4/ 0.7, 1.3/ 1.6, 3.1	0.5, 0.6/ 0.2, 0.4	34.8, 68.8 (E/T=5, 48 hrs)
GF-CART03 Multiple Solid Tumors	7.3	iCasp9-CAR Modulator 1 + Modulator 2	12.4~27.0 (n=3)	35~253	1.3~1.9	60.9~85.9/ 49.3~73.5	1.1~6.0/ 1.4~5.7/ 1.6~3.9	0.5~0.9/ 0.9~5.4	79.9~97.6 (E/T=5, 48 hrs)
	7.7	Modulator 1 + Modulator 2 + iCasp9-CAR	11.9, 14.7 (n=2)	25, 175	1.1, 2.3	88.5, 94.7/ 85.6, 87.3	0.7, 2.6/ 0.8, 3.5/ 1.1, 3.4	0, 0.9/ 1.6, 3.7	79.9, 85.9 (E/T=5, 48 hrs)
GF-CART04 Multiple Solid Tumors	6.1	iCasp9-CAR + Modulator 1	19.2 (n=1)	38	2.5	73.7/ 56.8	- / 31.1/ 14	- / 11.3	60.2 (E/T=1, 48 hrs)
	5.1	iCasp9-CAR + Modulator 2	30.7 (n=1)	139	1.9	78.8/ 62.6	- / 13.3/ 3.7	- / 1.1	66.0 (E/T=1, 48 hrs)

343

344

345 Importantly, we observed no obvious effect of transgene size on the
346 percentage of T_{SCM} cells, which remains the major population in both $CD4^+$ or $CD8^+$
347 T cell subtypes. Furthermore, in a ten-day culture, using the G-Rex setup with
348 *iCellar*™ supplementation, the production of clinical scale (up to 10E9) CAR^+
349 T_N/T_{SCM} cells in one liter of culture can still be achieved (data not shown).
350 Together, these results demonstrate that irrespective of gene identity and size,

performance of *qCART*™-produced T cells is still within satisfactory range. It also lends support to the feasibility of producing multiplexed CAR-T cells for clinical application. It should be noted that the observed downregulation of CAR expression may be due to multiple factors and further experimentation is needed to determine the exact mechanism. Nevertheless, it is important to point out that using the G-Rex setup, we do not observe as dramatic a drop in expression as that seen in virus-transduced CAR-T cells when its payload limit has been reached.

qCART™ system addresses unmet needs of conventional CAR-T therapies

As evidenced above, *qCART*™ overcomes major hurdles faced by current virus-based and virus-free genetic engineering and cell production systems. A schematic depiction of *qCART*™ summarizing and highlighting the roles of each platform is shown in Figure 6.

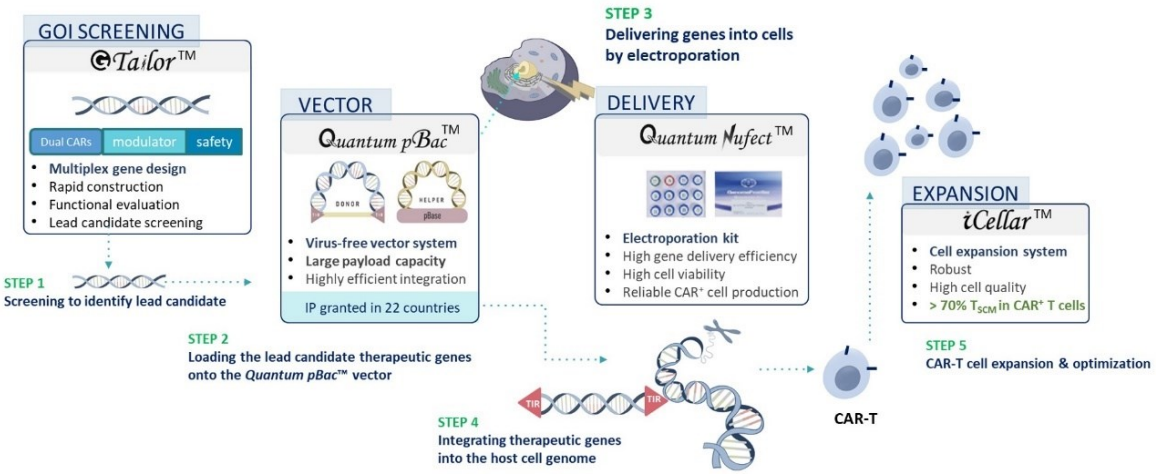

Figure 6. The _qCART_™ system

A schematic depiction showing the components of the *qCART*™ system.

375 **Discussion**

376 In this study, we have shown that the *qCART*™ system (Figure 6) effectively
377 and robustly produces CAR-T cells having qualities and in quantities that are
378 desirable for clinical application. We have shown that *GTailor*™ is an efficient
379 multiplex gene design and construct screening platform for designing CAR-T cells
380 with (i) the ability to recognize multiple targets; (ii) modulators for enhancing CAR-
381 T trafficking, infiltration and/or TME resistance; and (iii) a safety switch to terminate
382 the treatment as needed. We also demonstrated that the *qNF* platform is an
383 electroporation-based buffer for introducing therapeutic genes into T cells while
384 preserving cell viability. We previously demonstrated that the *qPB* platform is a
385 virus-free transposon vector system that: (i) possesses a large payload capacity,
386 (ii) is highly efficient in mediating genome integration, and (iii) has high preference
387 for T_{SCM} transposition.[24] Finally, we showed that *iCellar*™ is a cell expansion
388 platform for producing clinical-scaled CAR-T cells with (i) high percentage of CAR^+
389 T_{SCM} cells and (ii) enhanced fitness. In sum, we demonstrated that *qCAR-T*™ is a
390 streamlined, economic, and robust cell engineering system that expedites the
391 development and manufacturing of virus-free multiplex CAR-T therapy.

392 To date, the success achieved by CAR-T therapy in B cell lymphomas has
393 not been replicated in solid tumors.[34–36] The lack of cancer-specific antigens and
394 the immunosuppressive tumor microenvironment are major challenges blocking
395 success in solid tumor. One strategy to overcome these challenges is to engineer
396 T cells to simultaneously express multiple therapeutic genes. This can be
397 achieved using a technology capable of performing one-step multiplex gene

398 integration via a single cargo. Given the complexity of solid tumors and the distinct
399 attributes for each cancer type, a library of CAR-T cells encompassing a large
400 repertoire of GOI designs should be screened to identify the most suitable CAR
401 design. Furthermore, a system for rapid assessment of CAR-T cells' targeting
402 specificity and On-Target Off-Tumor toxicities is also needed. Lastly, high-
403 throughput cytotoxicity assays to identify the most efficacious CAR-T cell
404 candidates is crucial. *GTailor*™, the R&D component of the *qCART*™ system,
405 addresses all of the aforementioned needs. It streamlines the process for
406 identifying the most optimal multiplex gene design that can be tailored to combat
407 a variety of cancer types.

408 Consistency during production and in products is the most desirable
409 manufacturing attribute. By applying *qCART*™ in small-scale CAR-T cell
410 production, high quality CAR-T products with low batch-to-batch and inter-donor
411 variations are routinely obtained. *qCART*™ is able to achieve consistency due to
412 two reasons. The first includes the highly effective transfection, chromosomal
413 transposition, as well as cell expansion during CAR-T cell production process. The
414 second is that the CAR-T product possesses all of the desired features, including
415 reduced safety risks, identity, purity, and potency. The CD19/CD20 tandem CAR-
416 T with iCasp9 is an exemplary product which possesses all of these desired
417 features.[26] Possible mechanisms that contribute to the desired high CAR-T_{SCM},
418 balanced CD8:CD4 ratio, and reduced safety concerns are discussed below.

419 A transfection reagent capable of achieving high-efficiency gene delivery
420 with minimal toxicity is imperative for producing reliable gene-modified cell

421 products. We show in this study that, compared to HTCN, nucleofection using *qNF*
422 is a gentler combination that resulted in higher percentages of viable T cells having
423 enhanced expansion capacity (Figures 2 and 3), and higher numbers of CAR-T
424 cells produced (Figure 3). In addition to the known toxic effects of excess DNA[37]
425 which may contribute to the lower viability of HTCN-transfected CAR-T cells, the
426 observed discrepancy in CAR-T cell production between *qNF- and* HTCN-
427 transfected CAR-T cells may be caused by differential levels of CAR expression.
428 Previous studies have found that high CAR expression on the T cell surface can
429 result in spontaneous antigen-independent clustering of CAR and produce tonic
430 signaling that result in impaired expansion and apoptosis/exhaustion of the
431 cells.[38,39] In line with this finding, we found that the majority of live HTCN-
432 transfected T cells expressed the transgene at markedly higher (MFI) levels
433 compared with those of *qNF*-transfected T cells (10E2-10E4 and 10E1-10E3,
434 respectively; Figure 2A).[37] The higher level of CAR expression in HTCN-
435 transfected T cells may have caused greater cellular toxicity, reduced cell survival
436 and subsequent lower CAR-T expansion.[32] Conversely, the lower CAR expression
437 levels in *qNF*-transfected cells may result in: (1) greater CAR-T cell survival due to
438 reduced toxicity of either DNA or tonic signaling and/or electroporation-induced
439 death and (2) greater CAR^+ T cell expansion due to lower cell damage after
440 electroporation. The lower transfection rate by *qNF* as compared to HTCN is
441 rescued by *qPB*'s superior gene integration efficiency. Thus, *qNF* and *qPB*
442 platforms cooperate to enrich for CAR^+ T cells.

443 Risks associated with random gene integration represent a major safety
444 concern in gene therapy. A recent clinical report demonstrated that 2 of 10 patients
445 treated with *piggyBac*-modified CD19 CAR-T therapy developed CAR-T-cell
446 lymphoma.[40] A detailed mechanistic study on the case revealed a high number of
447 *piggyBac* integrants, but none were inserted into or near typical oncogenes.[41]
448 Nevertheless, this study highlights the importance of keeping a low copy number
449 of integrants per genome in gene therapy products. Of note, the study found
450 transgene integration into (introns of) the *BACH2* gene in both malignancies, which
451 we also found in CAR-T cells derived from one of two donors included in the
452 present study (Table S3). However, the study went on to conclude that *BACH2*
453 integration is unlikely to be playing a role in malignant behavior, in part due to
454 *BACH2* also being a recurrent insertion site for retroviruses.[41]

455 Our previous study has demonstrated that *qPB* is the most effective
456 *piggyBac*-based transposon system for engineering CAR-T cells.[24] Here, we have
457 further confirmed that *qPB* is a potentially safe vector for producing clinical-grade
458 CAR-T cells given its low copy number of integrant (<5 copies per cell) and similar
459 integration site biodistribution profile compared with other gene engineering and
460 production systems. Furthermore, as compared to *hyPB*, *qPB* leaves behind
461 significantly lower amount of backbone residues on the genome (107 bp vs. ~600
462 bp) and lacks the dominant enhancer activity found in backbone residues of *hyPB*,
463 thereby making it a relatively safer *piggyBac* system for CAR-T cell production.[24]

464 Naïve T cells (T_N) and T_{SCM} have the capacity to persist in cancer patients,
465 leading to improved clinical outcome.[42] Hence, enriching these cell types,

466 especially CAR$^+$ T_{SCM} cells, has become a central focus in the development of
467 next-generation CAR-T therapy.[17–20] Our studies have demonstrated that almost
468 all *qCART*™-generated CAR-T cell products contain >90% T_N and T_{SCM} (> 70%
469 T_{SCM} in most cases) in both CD4 and CD8 CAR$^+$ T cell populations, regardless of
470 (1) CAR construct design, (2) GOI size, and (3) PBMC source (healthy donors or
471 patients with B-cell malignancies; Figure 4, Table 2).[26] We believe this desired
472 feature is synergistically achieved by the combined benefits derived from: (1)
473 including 4-1BB rather than CD28 in the CAR construct, (2) using *qNF* instead of
474 HTCN for nucleofection, (3) choosing *qPB* over virus-based or other virus-free (e.g.
475 *hyPB*) vector systems, and (4) using *iCellar*™, *qBT* in particular, for CAR-T cell
476 expansion. Possible mechanisms that may contribute to the high CAR-T_{SCM}
477 enrichment in our CAR-T products include, first, it has been demonstrated that 4-
478 1BB signaling in CAR-T cells promotes T_{SCM} expansion, whereas CD28 favors T_{EFF}
479 expansion.[43] Second, the magnitude of reduction in cell expansion capacity
480 associated with electroporation-induced damage (Figure 2C) may be amplified in
481 highly proliferating cells such as T_{SCM}. Third, extended *ex vivo* expansion of virus-
482 based CAR-T cells often resulted in more differentiated T_{EFF} phenotype with higher
483 expression of exhaustion markers, such as TIM3 and PD1. In contrast, when *ex*
484 *vivo*-cultured for the same time-frame, *piggyBac*-based CAR-T products
485 consistently have >70% of T_{SCM}, which may be further enhanced by using *qPB*
486 rather than *hyPB* as the gene engineering vector system. Finally, current *ex vivo*
487 approaches to expand CAR-T cells to sufficient numbers while maintaining a
488 minimally-differentiated phenotype are hindered by the biological coupling of clonal

489 expansion and effector differentiation. In this study, we demonstrated that *qBT*, a
490 component of *iCellar*™, not only promoted robust CAR-T cell expansion but also
491 maintained T cell stemness even in the presence of antigen-expressing aAPC.
492 One possibility is that *qBT* increased the CD4 CAR^+ T_{SCM} population (Figure 4C),
493 which in turn enhanced proliferation of CD8 T_{SCM} population without concomitant
494 differentiation. This may reflect the high (3-9) and balanced (approximately 1)[26]
495 CD8:CD4 ratios observed in healthy donors and patients, respectively.

496 Since its first clinical study publication in 2016,[44] the so called "off-the-shelf"
497 allogeneic CAR-T therapy has been thought of as an inevitable replacement of
498 autologous CAR-T products. However, ample clinical data have concluded that
499 allogeneic CAR-T products are less potent and limited in CAR-T cell persistence
500 as compared to their autologous counterpart. In October 2021, the FDA placed a
501 clinical hold on all Allogene Therapeutics' AlloCAR-T clinical trials after a
502 chromosomal abnormality was found in a patient who received the anti-CD19
503 allogeneic CAR-T therapy. The incident further raised concerns regarding all
504 allogeneic CAR-T therapies. Induced pluripotent stem cells (iPSC)-derived CAR-
505 T cells may be a promising alternative for allogeneic CAR-T therapy. However,
506 such approaches are at an early stage of development and require further pre-
507 clinical and clinical research. Furthermore, the heavy mutation burden of iPSCs
508 poses safety concerns regarding its clinical applications. Thus, autologous CAR-
509 T therapy is likely to remain the mainstay of CAR-T based treatment, at least in the
510 short to medium term. In this regard, we have demonstrated that *qCART*™
511 addressed most if not all of the current challenges of autologous CAR-T therapy.

512 Thus, we expect this streamlined, robust, and virus-free cell engineering system
513 to unlock the full potential of CAR-T therapy for treating diseases.
514

515 **Materials and Methods**

516 **Human T cell samples from healthy donors**

517 Blood samples from adult healthy donors were obtained from Chang Gung
518 Memorial Hospital (Linkou, Taiwan), the acquisition of these samples was
519 approved by the Institution Review Board (IRB No. 201900578A3) at Chang Gung
520 Medical Foundation.

521 ***GTailor*™ identification of lead candidates**

522 A proprietary collection of primary cells and (engineered) cell lines were
523 used for *in vitro* evaluation of ON-Target anti-tumor activities. Stable cell lines
524 engineered to express a reporter gene (luciferase and/or GFP or tdTomato) were
525 generated using either a *piggyBac* or a lentivirus vector system. A proprietary
526 collection of parental plasmids of various configurations were used to generate a
527 library of constructs, and the indicated gene(s) of interest (GOI) of various identities
528 and sizes were cloned into the construct's multiple cloning site. *qPB* parental
529 donor plasmids carrying the indicated GOI were used to construct minicircle DNA
530 using methodology as previously described.[45] CAR-T cells produced by
531 nucleofection of activated T cells with these minicircle donor constructs in
532 combination with a *Quantum PBase* helper plasmid (i.e. *qPB*) were evaluated for
533 their performance as well as their *in vitro* cytotoxic activity against the collection of

534 cells. Once a lead candidate is identified, its *in vivo* antitumor activity is also
535 evaluated in a mouse xenograft model.

536 **Mapping of *Quantum pBac*™ genome integration sites (IS)**

537 Genomic DNA of CAR-T products was extracted using DNeasy Blood and
538 Tissue Kit (QIAGEN, Germantown, MD) and randomly fragmented (<500 bp
539 fragments) using a Bioruptor® Pico sonication device (Diagenode, Denville, NJ).
540 The fragments were ligated to adapters, purified using AMPure XP beads
541 (Beckman Coulter, Indianapolis, IN), and amplified by PCR. The amplified
542 products with an end sequence of the CAR gene were further amplified by PCR.
543 The final PCR products were subjected to sequencing using NovaSeq system
544 (Illumina, San Diego, CA).

545 Following sequencing, adapter and molecular barcode sequences were removed
546 from the raw reads sequencing data using the Agilent Genomics NextGen Toolkit
547 (AgeNT) software module (Agilent, Santa Clara, CA). The reads were then aligned
548 to the hg38 human genome using Burrows–Wheeler aligner (version 0.7.17-
549 r1188)[46] and the mapping results sorted using SAMtools (version 1.9).[47] IS were
550 manually identified using Genome Rearrangement Identification Software Suite
551 (GRIDSS)[48] and BEDTools (version 2.30.0).[48] For analysis of IS in proximity to
552 cancer-associated genes, reads data was compared with cancer gene database
553 downloaded from Cancer Hotspots (https://www.cancerhotspots.org/). The next
554 generation sequencing raw data set is shown in Supplementary Table S7.

555 **Generation and expansion of CAR-T cells**

556 Peripheral blood mononuclear cells (PBMCs) were isolated from blood
557 samples of healthy donors utilizing Ficoll-Hypaque gradient separation. $CD3^+$ T
558 cells were isolated from PBMCs using EasySep™ Human T Cell Isolation Kit
559 (StemCell Technologies, Taiwan) according to the manufacturer's instructions. T
560 cells were activated by co-incubation with Dynabeads™ (ThermoFisher Scientific,
561 Hillsboro, OR) for two days at a beads-to-cells ratio of 3:1. Following the removal
562 of Dynabeads™, activated T cells were subjected to nucleofection with a minicircle
563 CAR donor construct and a *Quantum PBase*™ plasmid (i.e. *qPB*) using a
564 Nucleofector™ 2b or 4D Device (Lonza, Morrisville, NC) in combination with either
565 the Amaxa® Human T Cell Nucleofector® Kit (Lonza) or the *qNF* Kit
566 (GenomeFrontier Therapeutics Inc., Taiwan), as according to the respective
567 manufacturer's instructions. Nucleofected cells were cultured for 10 or 12 days in
568 OpTmizer medium (Thermo Fisher) supplemented with *qBT* (GenomeFrontier
569 Therapeutics, Taiwan)(and aAPC) in G-Rex 24- or 6M-well plates (Wilson Wolf;
570 "G-Rex setup) or conventional plates ("Perfusion setup"), and then harvested for
571 analysis/further experiments. In experiments assessing the effect of cell viability
572 on expansion capacity, T cells were nucleofected using different program settings
573 (Nucleofector™ 2b) and cultured for four days in OpTmizer medium (Thermo
574 Fisher Scientific, Hillsboro, OR) supplemented with 50 IU of IL-2 (PeproTech,
575 Cranbury, NJ) and 10% FBS (Caisson Technologies, Seattle, WA). In experiments
576 involving the addition of aAPC, γ-irradiated aAPC were added on Day 3 to T cells
577 at a 1:1 aAPC:T cell ratio. T cells with or without addition of aAPC were cultured

578 in OpTmizer medium, supplemented with 50 IU of IL-2 and 10% FBS or *qBT*
579 (GenomeFrontier Therapeutics Inc., Taiwan).

580 **Evaluation of CAR-T cell performance**

581 Unless otherwise specified, flow cytometry analysis performed on a SA3800
582 Spectral Analyzer (Sony Biotechnology, San Jose, CA) was used to determine the
583 following: CAR expression on T cells was determined by staining with $F(ab')_2$
584 fragment specific, biotin-conjugated goat anti-mouse antibodies (Jackson
585 ImmunoResearch Laboratories, West Grove, PA), and R-phycoerythrin (PE)-
586 conjugated streptavidin (Jackson ImmunoResearch Laboratories, West Grove,
587 PA). Cells were also stained with one or more of the following antibodies: CD3-
588 Pacific Blue, CD4-Alexa Flour 532 (ThermoFisher Scientific, Hillsboro, OR), CD8-
589 PE-Cy7, CD45RA-BV421, CD62L-PE-Cy5, and CD95-BV711 (Biolegend, San
590 Diego, CA). For determination of live cells, cells were incubated with propidium
591 iodide (PI, Thermo Fisher Scientific, Hillsboro, OR) and/or Acridine orange (AO,
592 Nexcelom, Lawrence, MA). T cell subsets were determined based on CD45RA,
593 CD62L and CD95 staining: T_N ($CD45RA^+CD62L^+CD95^-$), T_{SCM}
594 ($CD45RA^+CD62L^+CD95^+$), T_{CM} ($CD45RA^-CD62L^+$), T_{EM} ($CD45RA^-CD62L^-$), and
595 T_{EFF} ($CD45RA^+CD62L^-$). Histograms and dot-plots were generated using
596 GraphPad Prism software (GraphPad Software, San Diego, CA). Total day 1 live
597 cells were determined using Celigo image cytometry (Nexcelom, Lawrence, MA)
598 and represent the number of AO^+, PI^- cells. Viability index was calculated using
599 the formula: (AO^+, PI^- live cells on day 1/total number of electroporated cells) x 100.

600 Number of CAR^+ live cells was calculated according to the formula: Total day 1
601 live cells x percentage of CAR^+ of live cells.

602 ***In vivo* cytokine release assay**

603 Mouse serum samples were collected on Days 3, 15, 29 and 43 following T
604 cell injection. Serum levels of interferon gamma (IFN-γ) was measured by
605 performing enzyme-linked immunosorbent assay (Thermo Fisher Scientific,
606 Hillsboro, OR) according to the manufacturer's instructions.

607 ***In vitro* cytotoxicity assay**

608 $5x10^3$ cells per well of Raji-GFP/Luc target cells were seeded in 96-well
609 culture plates (Corning, Glendale, AZ) and CAR-T cells were added at an E:T ratio
610 of 1:1. CAR-T cell-mediated cytotoxicity on Raji-GFP/Luc target cells was then
611 assessed by using Celigo image cytometry (Nexcelom, Lawrence, MA) as
612 reported[49] to determine the number of live Raji-GFP/Luc cells at 0, 24, 48, 72 and
613 96 hours after co-culturing. Cell aggregates were separated by pipetting before
614 Celigo imaging. The percentage of specific lysis for each sample was calculated
615 using the formula: [1-(live fluorescent cell count in the presence of Raji-GFP/Luc
616 cells and CAR-T cells / live fluorescent cell count in the presence of Raji-GFP/Luc
617 cells only)] x 100.

618 **Mouse xenograft model**

619 *In vivo* studies using mouse xenograft model were conducted at the
620 Development Center for Biotechnology, Taiwan, using animal protocols approved
621 by the Taiwan Mouse Clinic IACUC (2020-R501-035). Briefly, eight-week-old
622 female ASID (NOD.Cg-Prkdc^{scid}Il2rg^{tm1Wjl}/YckNarl) mice (National Laboratory

623 Animal Center, Taiwan) were intravenously (i.v.) injected with 1.5×10^5 Raji-
624 GFP/Luc tumor cells. One week after Raji-GFP/Luc tumor cell injection, mice were
625 injected with $3\text{x}10^6$ CAR-T cells or control Pan-T cells (non-transfected T cells).
626 Luminescence signals from Raji-GFP/Luc tumor cells were monitored using the
627 Xenogen-IVIS Imaging System (Caliper Life Sciences, Hopkinton, MA).

628 **Genomic DNA extraction and quantitative PCR (qPCR)**

629 Genomic DNA from mouse blood was extracted using DNeasy Blood &
630 Tissue Kit (Qiagen, Germantown, MD) following the manufacturer's instructions.
631 7500 fast real-time PCR system (Applied Biosystems, Foster City, CA) was used
632 to carry out quantitative PCR analysis. Amplification of CAR gene (CAR-T cells)
633 and Luc gene (Raji-GFP/Luc cells) in mouse blood samples was carried out using
634 the CAR forward (5'-ACGTCGTACTCTTCCCGTCT-3') and reverse (5'-
635 GATCACCCTGTAC-TGCAACCA-3') primers and the luciferase forward (5'-
636 GGACTTGGACACCGGTAAGA-3')& reverse (5'-GGTCCACGATGAAGAAGTGC-
637 3') primers, respectively. The amount of CAR and Luc genes, expressed as gene
638 copy/ng of DNA, were calculated utilizing the standard curve method as previously
639 described.[50]

640 **Statistical analysis**

641 Statistical analyses of differences between two groups and among three or
642 more groups were carried out using the Student's t-test (two-tailed) and the one-
643 way ANOVA with Tukey's multiple comparison test, respectively. The analyses
644 were performed using Prism 7.0 (GraphPad Software, San Diego, CA), and
645 statistical significance was reported as * $p<0.05$, ** $p<0.01$, and *** $p<0.001$.

Acknowledgments

The authors thank Ms. Yi-Shan Yu and Ms. Lu-Chun Chen for their assistance throughout the IRB preparation and approval process. The authors also thank Dr. Pei-Yi Tsai for assistance with the animal experiments. This study is funded by GenomeFrontier Therapeutics, Inc.

Author Contributions:

S.C.-Y.W. designed research. Y.-C.C., W.-K.H., Y.-W.H., J.-C.T., Y.-H.K., P.-H.W., P.-N.W., K.-F.C., W.-T.L. performed research. J.C.H., Y.-C.C, W.-K.H., K.-L.K.W., and S.C.-Y.W. analyzed data. J.C.H., P.S.C. and S.C.-Y.W. wrote the paper.

Declaration of Interests Statement:

S.C.-Y.W. is the founder of GenomeFrontier Therapeutics, Inc., Y.-C.C., W.-K.H., K.-L.K.W., Y.-W.H., J.-C.T., Y.-H.K., P.-H.W., K.-F.C., W.-T.L., P.S.C. and J.C.H. are affiliated with GenomeFrontier Therapeutics, Inc.

664 ## References

665 1. Akkın, S., Varan, G., and Bilensoy, E. (2021). A review on cancer
666 immunotherapy and applications of nanotechnology to
667 chemoimmunotherapy of different cancers. Molecules *26*.

668 2. Waldman, A.D., Fritz, J.M., and Lenardo, M.J. (2020). A guide to cancer
669 immunotherapy: from T cell basic science to clinical practice. Nature
670 Reviews Immunology *20*.

671 3. June, C.H., and Sadelain, M. (2018). Chimeric Antigen Receptor Therapy.
672 New England Journal of Medicine *379*, 64–73.

673 4. Srivastava, S., and Riddell, S.R. (2015). Engineering CAR-T cells: Design
674 concepts. Trends in Immunology *36*.

675 5. Cappell, K.M., and Kochenderfer, J.N. (2021). A comparison of chimeric
676 antigen receptors containing CD28 versus 4-1BB costimulatory domains.
677 Nature Reviews Clinical Oncology *18*.

678 6. Marofi, F., Motavalli, R., Safonov, V.A., Thangavelu, L., Yumashev, A.V.,
679 Alexander, M., Shomali, N., Chartrand, M.S., Pathak, Y., Jarahian, M., et al.
680 (2021). CAR T cells in solid tumors: challenges and opportunities. Stem Cell
681 Research and Therapy *12*.

682 7. Patel PharmD, U., Abernathy, J.M., Savani, B.N., Oluwole, O.,
683 Sengsayadeth, S., Dholaria, B., Bhagirathbhai Dholaria, C., and pro-fessor,
684 A. (2021). CAR T cell therapy in solid tumors: A review of current clinical
685 trials.

686 8. Zhang, Z. zheng, Wang, T., Wang, X. feng, Zhang, Y. qing, Song, S. xia, and
687 Ma, C. qing (2022). Improving the ability of CAR-T cells to hit solid tumors:
688 Challenges and strategies. Pharmacological Research *175*.

689 9. Yeku, O.O., Purdon, T.J., Koneru, M., Spriggs, D., and Brentjens, R.J. (2017).
690 Armored CAR T cells enhance antitumor efficacy and overcome the tumor
691 microenvironment. Scientific Reports *7*.

692 10. Hawkins, E.R., D'souza, R.R., and Klampatsa, A. (2021). Armored CAR T-
693 cells: The next chapter in T-cell cancer immunotherapy. Biologics: Targets
694 and Therapy *15*.

695 11. Adachi, K., Kano, Y., Nagai, T., Okuyama, N., Sakoda, Y., and Tamada, K.
696 (2018). IL-7 and CCL19 expression in CAR-T cells improves immune cell
697 infiltration and CAR-T cell survival in the tumor. Nature Biotechnology *36*.

698 12. Zhou, J.T., Liu, J.H., Song, T.T., Ma, B., Amidula, N., and Bai, C. (2020).
699 EGLIF-CAR-T cells secreting PD-1 blocking antibodies significantly mediate
700 the elimination of gastric cancer. Cancer Management and Research *12*.

701 13. Ping, Y., Li, F., Nan, S., Zhang, D., Shi, X., Shan, J., and Zhang, Y. (2020).
702 Augmenting the Effectiveness of CAR-T Cells by Enhanced Self-Delivery of
703 PD-1-Neutralizing scFv. Frontiers in Cell and Developmental Biology *8*.

704 14. Suarez, E.R., Chang, D.K., Sun, J., Sui, J., Freeman, G.J., Signoretti, S., Zhu,
705 Q., and Marasco, W.A. (2016). Chimeric antigen receptor T cells secreting
706 anti-PD-L1 antibodies more effectively regress renal cell carcinoma in a
707 humanized mouse model. Oncotarget *7*.

708 15. Choi, B.D., Yu, X., Castano, A.P., Bouffard, A.A., Schmidts, A., Larson, R.C.,
709 Bailey, S.R., Boroughs, A.C., Frigault, M.J., Leick, M.B., et al. (2019). CAR-T
710 cells secreting BiTEs circumvent antigen escape without detectable
711 toxicity. Nature Biotechnology *37*.

712 16. Gattinoni, L., Lugli, E., Ji, Y., Pos, Z., Paulos, C.M., Quigley, M.F., Almeida,
713 J.R., Gostick, E., Yu, Z., Carpenito, C., et al. (2011). A human memory T cell
714 subset with stem cell-like properties. Nature Medicine *17*.

715 17. Arcangeli, S., Falcone, L., Camisa, B., de Girardi, F., Biondi, M., Giglio, F.,
716 Ciceri, F., Bonini, C., Bondanza, A., and Casucci, M. (2020). Next-Generation
717 Manufacturing Protocols Enriching TSCM CAR T Cells Can Overcome
718 Disease-Specific T Cell Defects in Cancer Patients. Frontiers in Immunology
719 *11*.

720 18. Zhang, M., Jin, X., Sun, R., Xiong, X., Wang, J., Xie, D., and Zhao, M.F.
721 (2021). Optimization of metabolism to improve efficacy during CAR-T cell
722 manufacturing. Journal of Translational Medicine *19*.

723 19. Fu, C., Shi, G., and Liu, Y.-T. (2021). Manufacturing Anti-CD19 CAR-Tscm
724 Cells for Immunotherapy Using Innovative Microbubble-Based
725 Technologies for Precision Cell Processing. Blood *138*.

726 20. Ronald Funk, C., Wang, S., Chen, K.Z., Waller, A., Sharma, A., Edgar, C.L.,
727 Gupta, V.A., Chandrakasan, S., Zoine, J.T., Fedanov, A., et al. (2022).
728 PI3Kd/g inhibition promotes human CART cell epigenetic and metabolic
729 reprogramming to enhance antitumor cytotoxicity.

730 21. Morgan, R.A., and Boyerinas, B. (2016). Genetic modification of T cells.
731 Biomedicines *4*.

732 22. Bulcha, J.T., Wang, Y., Ma, H., Tai, P.W.L., and Gao, G. (2021). Viral vector
733 platforms within the gene therapy landscape. Signal Transduction and
734 Targeted Therapy *6*.

735 23. Magnani, C.F., Gaipa, G., Lussana, F., Belotti, D., Gritti, G., Napolitano, S.,
736 Matera, G., Cabiati, B., Buracchi, C., Borleri, G., et al. (2020). Sleeping
737 Beauty–engineered CAR T cells achieve antileukemic activity without
738 severe toxicities. Journal of Clinical Investigation *130*, 6021–6033.

739 24. Hua, W.-K., Hsu, J.C., Chen, Y.-C., Chang, P.S., Wen, K.K.-L., Wang, P.-N., Yu,
740 Y.-S., Chen, Y.-C., Cheng, I.-C., and Wu, S.C.-Y. (2022). Quantum pBac: An
741 effective, high-capacity piggyBac-based gene integration vector system for
742 unlocking gene therapy potential.
743 https://doi.org/10.1101/2022.04.29.490002.

744 25. Meir, Y.J.J., Lin, A., Huang, M.F., Lin, J.R., Weirauch, M.T., Chou, H.C., Lin,
745 S.J.A., and Wu, S.C.Y. (2013). A versatile, highly efficient, and potentially
746 safer piggyBac transposon system for mammalian genome manipulations.
747 FASEB Journal *27*, 4429–4443.

748 26. Chang, P.S., Chen, Y.-C., Hua, W.-K., Hsu, J.C., Tsai, J.-C., Huang, Y.-W., Kao,
749 Y.-H., Wu, P.-H., Chang, Y.-F., Chang, M.-C., et al. (2022). Manufacturing
750 highly potent CD20/CD19-targeted iCasp9 regulatable CAR-T cells using the
751 Quantum pBac-based CAR-T (qCART) system for clinical application.
752 https://doi.org/10.1101/2022.05.03.490475.

753 27. Hamada, M., Nishio, N., Okuno, Y., Suzuki, S., Kawashima, N., Muramatsu,
754 H., Tsubota, S., Wilson, M.H., Morita, D., Kataoka, S., et al. (2018).
755 Integration Mapping of piggyBac-Mediated CD19 Chimeric Antigen
756 Receptor T Cells Analyzed by Novel Tagmentation-Assisted PCR.
757 EBioMedicine *34*, 18–26.

758 28. Vavouri, T., and Lehner, B. (2012). Human genes with CpG island
759 promoters have a distinct transcription-associated chromatin organization.
760 Genome Biology *13*.

761 29. Ott, M.G., Schmidt, M., Schwarzwaelder, K., Stein, S., Siler, U., Koehl, U.,
762 Glimm, H., Kühlcke, K., Schilz, A., Kunkel, H., et al. (2006). Correction of X-
763 linked chronic granulomatous disease by gene therapy, augmented by
764 insertional activation of MDS1-EVI1, PRDM16 or SETBP1. Nature Medicine
765 *12*, 401–409.

766 30. Braun, C.J., Boztug, K., Paruzynski, A., Witzel, M., Schwarzer, A., Rothe, M.,
767 Modlich, U., Beier, R., Göhring, G., Steinemann, D., et al. (2014). Gene
768 therapy for Wiskott-Aldrich syndrome-long-term efficacy and genotoxicity.
769 Science Translational Medicine *6*.

770 31. Hacein-Bey-Abina, S., Garrigue, A., Wang, G.P., Soulier, J., Lim, A., Morillon,
771 E., Clappier, E., Caccavelli, L., Delabesse, E., Beldjord, K., et al. (2008).
772 Insertional oncogenesis in 4 patients after retrovirus-mediated gene
773 therapy of SCID-X1. Journal of Clinical Investigation *118*, 3132–3142.

774 32. Cavazzana-Calvo, M., Payen, E., Negre, O., Wang, G., Hehir, K., Fusil, F.,
775 Down, J., Denaro, M., Brady, T., Westerman, K., et al. (2010). Transfusion
776 independence and HMGA2 activation after gene therapy of human β-
777 thalassaemia. Nature *467*.

778 33. Kebriaei P, Singh H, Huls M, Figliola M, Bassett R, Olivares S, Jena B,
779 Dawson M, Kumaresan P, Su S, et al. (2016). The Journal of Clinical
780 Investigation.

781 34. Thistlethwaite, F.C., Gilham, D.E., Guest, R.D., Rothwell, D.G., Pillai, M.,
782 Burt, D.J., Byatte, A.J., Kirillova, N., Valle, J.W., Sharma, S.K., et al. (2017).
783 The clinical efficacy of first-generation carcinoembryonic antigen
784 (CEACAM5)-specific CAR T cells is limited by poor persistence and transient
785 pre-conditioning-dependent respiratory toxicity. Cancer Immunology,
786 Immunotherapy *66*.

787 35. Lamers, C.H.J., Sleijfer, S., van Steenbergen, S., van Elzakker, P., van
788 Krimpen, B., Groot, C., Vulto, A., den Bakker, M., Oosterwijk, E., Debets, R.,
789 et al. (2013). Treatment of metastatic renal cell carcinoma with CAIX CAR-
790 engineered T cells: Clinical evaluation and management of on-target
791 toxicity. Molecular Therapy *21*.

792 36. Brown, C.E., Badie, B., Barish, M.E., Weng, L., Ostberg, J.R., Chang, W.C.,
793 Naranjo, A., Starr, R., Wagner, J., Wright, C., et al. (2015). Bioactivity and
794 safety of IL13Rα2-redirected chimeric antigen receptor CD8+ T cells in
795 patients with recurrent glioblastoma. Clinical Cancer Research *21*.

796 37. Huerfano, S., Ryabchenko, B., and Forstová, J. (2013). Nucleofection of
797 expression vectors induces a robust interferon response and inhibition of
798 cell proliferation. DNA and Cell Biology *32*, 467–479.

799 38. Gomes-Silva, D., Mukherjee, M., Srinivasan, M., Krenciute, G., Dakhova, O.,
800 Zheng, Y., Cabral, J.M.S., Rooney, C.M., Orange, J.S., Brenner, M.K., et al.
801 (2017). Tonic 4-1BB Costimulation in Chimeric Antigen Receptors Impedes
802 T Cell Survival and Is Vector-Dependent. Cell Reports *21*, 17–26.

803 39. Long, A.H., Haso, W.M., Shern, J.F., Wanhainen, K.M., Murgai, M.,
804 Ingaramo, M., Smith, J.P., Walker, A.J., Kohler, M.E., Venkateshwara, V.R.,
805 et al. (2015). 4-1BB costimulation ameliorates T cell exhaustion induced by
806 tonic signaling of chimeric antigen receptors. Nature Medicine *21*.

807 40. Bishop, D.C., Clancy, L.E., Simms, R., Burgess, J., Mathew, G., Moezzi, L.,
808 Street, J.A., Sutrave, G., Atkins, E., McGuire, H.M., et al. (2021).
809 Development of CAR T-cell lymphoma in 2 of 10 patients effectively
810 treated with piggyBac-modified CD19 CAR T cells. Blood *138*.

811 41. Micklethwaite, K.P., Gowrishankar, K., Gloss, B.S., Li, Z., Street, J.A.,
812 Moezzi, L., Mach, M.A., Sutrave, G., Clancy, L.E., Bishop, D.C., et al. (2021).
813 Investigation of product-derived lymphoma following infusion of piggyBac-
814 modified CD19 chimeric antigen receptor T cells. Blood *138*.

815 42. Fraietta, J.A., Lacey, S.F., Orlando, E.J., Pruteanu-Malinici, I., Gohil, M.,
816 Lundh, S., Boesteanu, A.C., Wang, Y., O'connor, R.S., Hwang, W.T., et al.
817 (2018). Determinants of response and resistance to CD19 chimeric antigen

818 receptor (CAR) T cell therapy of chronic lymphocytic leukemia. Nature
819 Medicine *24*.

820 43. Kawalekar, O.U., O'Connor, R.S., Fraietta, J.A., Guo, L., McGettigan, S.E.,
821 Posey, A.D., Patel, P.R., Guedan, S., Scholler, J., Keith, B., et al. (2016).
822 Distinct Signaling of Coreceptors Regulates Specific Metabolism Pathways
823 and Impacts Memory Development in CAR T Cells. Immunity *44*.

824 44. Brudno, J.N., Somerville, R.P.T., Shi, V., Rose, J.J., Halverson, D.C., Fowler,
825 D.H., Gea-Banacloche, J.C., Pavletic, S.Z., Hickstein, D.D., Lu, T.L., et al.
826 (2016). Allogeneic T cells that express an anti-CD19 chimeric antigen
827 receptor induce remissions of B-cell malignancies that progress after
828 allogeneic hematopoietic stem-cell transplantation without causing graft-
829 versus-host disease. Journal of Clinical Oncology *34*.

830 45. Kay, M.A., He, C.Y., and Chen, Z.Y. (2010). A robust system for production
831 of minicircle DNA vectors. Nature Biotechnology *28*, 1287–1289.

832 46. Li, H. (2013). Aligning sequence reads, clone sequences and assembly
833 contigs with BWA-MEM.

834 47. Li, H., Handsaker, B., Wysoker, A., Fennell, T., Ruan, J., Homer, N., Marth,
835 G., Abecasis, G., and Durbin, R. (2009). The Sequence Alignment/Map
836 format and SAMtools. Bioinformatics *25*.

837 48. Cameron, D.L., Schröder, J., Penington, J.S., Do, H., Molania, R., Dobrovic,
838 A., Speed, T.P., and Papenfuss, A.T. (2017). GRIDSS: Sensitive and specific
839 genomic rearrangement detection using positional de Bruijn graph
840 assembly. Genome Research *27*.

841 49. Sun, Yu-Jun; Chen, Yi-Chun; Hua, Wei-Kai; Wu, Sareina C-Y; Chan, L. (2022).
842 Cytometry (*In press*).

843 50. Zhou, X., Shen, L., Liu, L., Wang, C., Qi, W., Zhao, A., Wu, X., and Li, B.
844 (2016). Preclinical safety evaluation of recombinant adeno-associated virus
845 2 vector encoding human tumor necrosis factor receptor-immunoglobulin
846 Fc fusion gene. Human Vaccines and Immunotherapeutics *12*.

847